European Journal of Pharmacology 588 (2008) 18–25

Contents lists available at ScienceDirect

European Journal of Pharmacology

journal homepage: www.elsevier.com/locate/ejphar

Catabolic attacks of membrane-bound angiotensin-converting enzyme on the N-terminal part of species-specific amyloid-β peptides

Xiaoou Sun [a,b], Matthias Becker [a], Kristin Pankow [a], Eberhard Krause [a], Martina Ringling [a], Michael Beyermann [a], Bjoern Maul [a], Thomas Walther [b], Wolf-Eberhard Siems [a,*]

[a] Leibniz-Institut für Molekulare Pharmakologie (FMP), D-13125 Berlin, Germany
[b] Department Cardiology, Charité, Campus Benjamin Franklin (CBF), D-12200 Berlin, Germany

ARTICLE INFO

Article history:
Received 8 August 2007
Received in revised form 14 March 2008
Accepted 31 March 2008
Available online 6 April 2008

Keywords:
Alzheimer's disease
Amyloid-β peptide (Aβ)
Angiotensin-converting enzyme (ACE)
Catalytic domains of ACE
Neprilysin (NEP)

ABSTRACT

Catabolic processes play a crucial role in the steady state of the amyloid-β peptide (Aβ). Neprilysin (NEP) and angiotensin-converting enzyme (ACE), two transmembranal enzymes with greatest importance in peptide pharmacology, are known to play a role in Aβ catabolism. This paper focuses on the N-terminal part of Aβ. This region contains the three amino acid residues that determine the differences between human (hAβ) and murine Aβ (mAβ). Moreover, the N-terminal part of Aβ contains the zinc-binding site of the molecule. Consequently, all hydrolytic attacks on this part of the Alzheimer peptide should be of exceptional interest. We investigated domain-selective forms of ACE in HPLC-monitored peptide degradation studies and used mass spectrometry for product analyses. We found that ACE-evoked a hydrolysis of the N-terminal part of m- and hAβ. The hAβ sequence hAβ (4–15) was found to be a better substrate for ACE compared to the corresponding murine form. Moreover, we localized the corresponding cleavage sites in the N-terminal part of Aβ as well as in the full-length molecule and identified new sites of endopeptidolytic attack by ACE. Finally, we demonstrate that both catalytic domains of mACE have similar hydrolytic activity on the N-terminal part of Aβ. Our results show that ACE besides its typical function as a dipeptidyl-carboxypeptidase has also unequivocal endopeptidolytic activities.

1. Introduction

According to the amyloid-hypothesis, the central concentration of the amyloid-β peptide (Aβ) plays a crucial role in the development of Alzheimer's disease. The fragile steady state of extracellular Aβ is strongly influenced by two different peptidolytic processes — anabolic (for review see Hardy and Selkoe, 2002) and catabolic actions (review see Saido and Iwata, 2006; Wang et al., 2006). Over the last years, scientific interest focused on the catabolic activity of several peptidases on Aβ. NEP (neprilysin or neutral endopeptidase, EC 3.4.24.11), ACE (angiotensin-converting enzyme, EC 3.4.15.1), IDE (insulin-degrading enzyme, EC 3.4.24.56), ECE (endothelin-converting enzyme, EC 3.4.24.71) and plasmin (EC3.4.21.7) are involved in these processes (for review see Wang et al., 2006). Interestingly, most of these enzymes play also important roles in non-neuronal processes, and substances that interfere with the function of these enzymes are used as therapeutics. For example, ACE, a transmembranal dipeptidyl-carboxypeptidase, is involved in several angiotensin- or bradykinin-triggered renal, vascular, and cardiac processes. Thus, potent and specific inhibitors of ACE have been widely used in the treatment of cardiovascular disease and for other therapeutic purposes and belong to the top-selling drugs.

The amino acid sequences of Aβ peptides were strongly conserved in evolution. However, the N-terminal parts of the murine and the human Aβ molecule contain species-specific amino acid sequences. Three distinct differences in the N-terminal part (position 5 [Arg/Gly], position 10 [Tyr/Phe], and position 13 [His/Arg]) have been discussed to be responsible for the almost complete absence of Aβ aggregation and deposition in mice (Vaughan and Peters, 1981). Especially, the both mentioned membrane-bound peptidases ACE and NEP have been reported to cleave the Aβ molecule initially in its N-terminal section (for review see Wang et al., 2006). The NEP-derived Aβ degradation is well described (Howell et al., 1995; Iwata et al., 2000; Yasojima et al., 2001; Mohajeri et al., 2004). Notably, Iwata et al. (2000) found that NEP cleaves the Aβ molecule in position 9–10, in which structural differences exist between human and murine Aβ. Hu et al. (2001) reported that ACE degrades hAβ by cleaving between Asp^{7}-Ser^{8}. This attracts further attention, because it was the first observation of a unequivocal endopeptidolytic activity of the 'dipeptidyl-carboxypeptidase' ACE.

* Corresponding author. Leibniz-Institut für Molekulare Pharmakologie (FMP), Robert-Roessle-Str. 10, D-13125 Berlin, Germany. Tel.: +49 30 94793251; fax: +49 30 94793250.
E-mail address: siems@fmp-berlin.de (W.-E. Siems).

0014-2999/$ – see front matter © 2008 Elsevier B.V. All rights reserved.
doi:10.1016/j.ejphar.2008.03.058

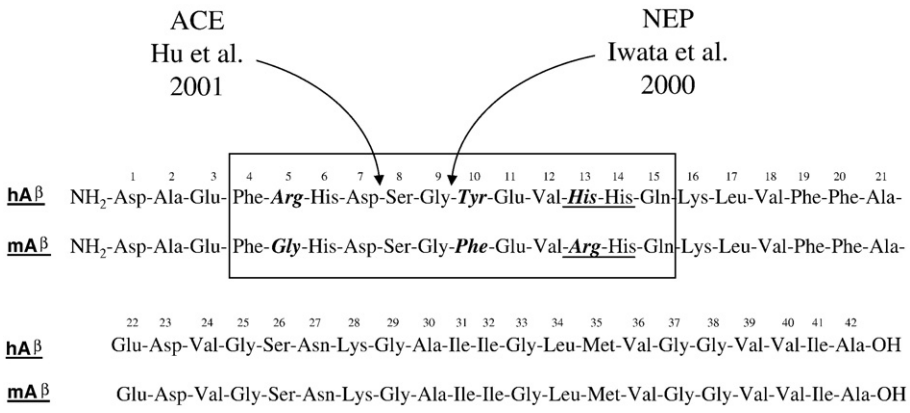

Fig. 1. Amino acid sequences of human (hAβ) and murine amyloid peptides (mAβ). Species-specific differences (human versus murine) are indicated in bold and Italics. Known N-terminal cleavage sites after NEP- (Iwata et al., 2000) and ACE-attacks (Hu et al., 2001) are indicated by arrows. Amino acids involved in Zn^{++} binding sites are underlined. The N-terminal sequences hAβ (4–15) and mAβ (4–15) are framed.

In addition to these structural and catabolic relations, the N-terminal part of Aβ plays further important roles. Especially, the histidyl residues in position 13 and 14 in hAβ are found to be important for Zn^{2+}-binding and for the Zn-induced aggregation of the peptide (Liu et al., 1999; Miura et al., 2000; Kozin et al., 2001). The importance of the N-terminal part of Aβ and its degradation is also underlined by experiments using specific antibodies that reduce the plaque burden in Alzheimer's disease. Antibodies against the N-terminus of Aβ are very effective, while antibodies against the C-terminus of Aβ were not (Yang et al., 2000a,b; Chauhan and Siegel, 2005).

Considering that full-length Aβ (especially its human form) is difficult to handle, we focused on peptide sequence Aβ (4–15) that has adequate solubility and does not display spontaneous formation of oligomeric structures and associates. Aβ (4–15) already contains the interesting parts of the Aβ molecule: the three species-specific structural modifications, the Zn^{2+}-binding amino acids, and the described ACE- and NEP-cleavage sites.

The major aim of this study was to compare the action of ACE on the structurally different N-terminal parts of murine and human Aβ, and to describe respective cleavage sites. ACE has two nearly identical catalytic domains (Wei et al., 1992; Jaspard et al., 1993) that in spite of their homology, have different substrate properties (Rousseau et al., 1995; Deddish et al., 1998; Araujo et al., 2000). Consequently, these studies were also set up to clarify whether and how the both catalytic domains of ACE, the C- and the N-domain, are differently involved in the peptidolytic cleavage of Aβ.

2. Materials and methods

2.1. Materials

mAβ (1–40), hAβ (1–40), mAβ (1–42), hAβ (1–42) and the corresponding N-terminal partial sequences mAβ (4–15), hAβ (4–15), were

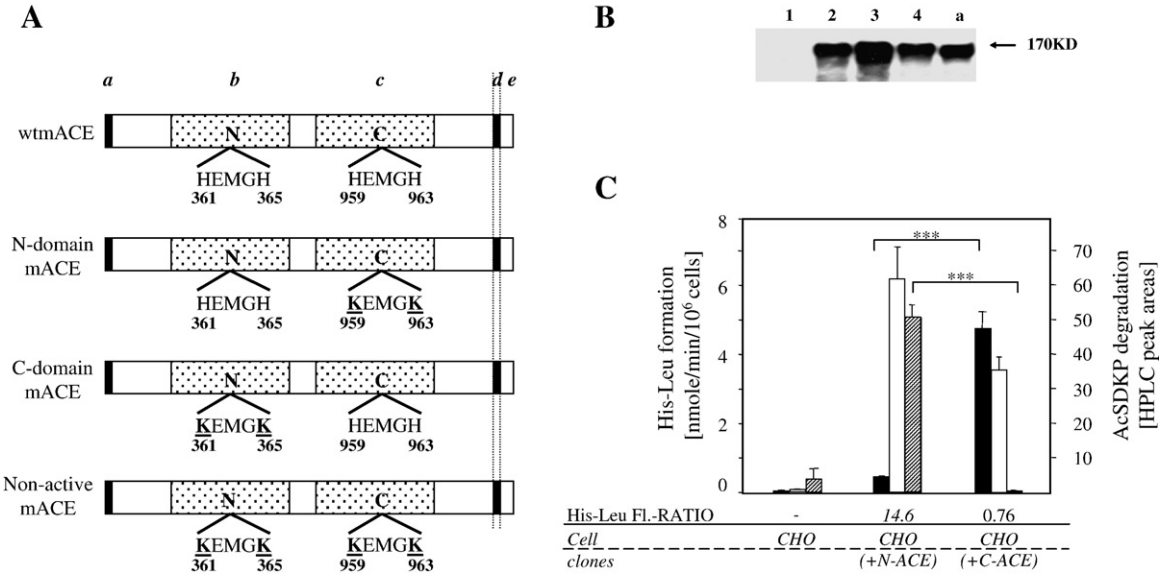

Fig. 2. Domain-selective forms of membrane-bound murine ACE (mACE), their molecular architecture, molecular mass and catalytic selectivity. (A) Schematic presentation of site-directed mutations in somatic murine ACE (mACE). Exchanged amino acids (His [H]versus Lys [K]) are underlined and in bold *Indicated ACE-segments*: (*a*) N-terminus; (*b*) catalytic N-domain; (*c*) catalytic C-domain; (*d*) transmembranal region; (*e*) C-terminus, cytoplasmatic tail; (*a–c*) extracellular parts. (B) Western blotting of the distinct forms of mACE expressed in CHO cells. (1) non-transfected CHO cells; (2) wtmACE-transfected CHO cells; (3) N-domain mACE-transfected CHO cells; (4) C-domain ACE-transfected CHO; as controls: (a) non-active ACE-transfected CHO cells. (C) ACE activities of selected domain-selective cell clones. CHO, non-transfected CHO cells; CHO (+N-ACE), N-domain mACE-transfected CHO cells; CHO (+C-ACE), C-domain mACE-transfected CHO cells. Used substrates (from left to right): Hip-His-Leu (black columns), Z-Phe-His-Leu (white columns), AcSDKP (hatched columns). Mean values with S.E.M., $n=5$. The significance of differences for the degradation of domain-selective substrates (AcSDKP and Hip-His-Leu) by N- versus C-domain mACE-transfected cells was proved by *t*-tests. ***$p>0.001$.

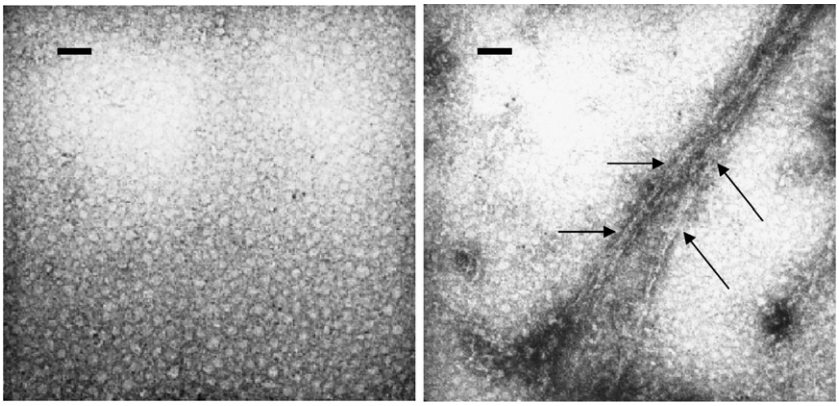

Fig. 3. Electron-microscopic analysis of in-vitro fibril formation. Solutions of purified full-length murine Aβ (1–42) (left) and human Aβ (1–42) (right) were incubated under conditions approximated to physiological. Preparation and electron-microscopic analysis were performed as described by Janek et al. (1999). The horizontal black lines correspond to 117 nm. Fibrils in B are indicated by arrows.

synthesized by M.B. (see also Fig. 1). Recombinant human ACE (rhACE) and murine ACE (rmACE) were obtained from R&D systems (Wiesbaden-Nordenstadt, Germany). Acetyl-Ser-Asp-Lys-Pro (AcSDKP), Hip-His-Leu, Z-Phe-His-Leu and Lisinopril were from Sigma-Aldrich (München, Germany). Polyclonal antibody raised against mACE was from Santa Cruz, Biotechnology Inc. (Heidelberg, Germany).

2.2. In-vitro fibril formation

Amyloid peptides were synthesized as described above. Peptides [mAβ (1–42), and hAβ (1–42)] were purified on a reverse phase HPLC C18 column, and thereafter characterized by mass spectrometry and automatic amino acid analysis. A 0.2-mM solution of h- and mAβ (1–42), respectively, solved in highly purified water containing 5% freshly distilled DMSO, was incubated at room temperature for 24 h and subsequently, subjected to a 300-mesh copper grid (carbon-covered), treated with 2% uranylacetate and dried. Further steps of preparation and electron-microscopic analysis, using a 902A electron microscope (Zeiss, Oberkochen, Germany) were performed as principally described by Janek et al. (1999).

2.3. Generation of plasmids containing somatic mACE and mACE mutants

A 4.1-kb BamHI/KpnI fragment of murine ACE cDNA, which contains the entire coding sequence for kidney ACE, was inserted into the expression vector pcDNA3.1 (Invitrogen GmbH, Karlsruhe, Germany) digested with BamHI and KpnI. The resulting plasmid was designated wtmACE. Site-specific mutations (Wei et al., 1991) were introduced into the respective active site of either the N- or the C-domain by using the "QuickChange Site-Directed Mutagenesis Kit" (Stratagene-Europe, Amsterdam, the Netherlands), whereby the C-domain mutation at the positions 361 and 365 (His to Lys) as well as the N-domain at positions 959 and 963 (His to Lys) were introduced into the recombinant plasmid containing the full-length cDNA sequence of mACE (Fig. 2A). The resulting plasmids were named C-domain mACE and N-domain mACE. The full-length and mutant cDNAs were finally checked by DNA sequencing (Invitek, Berlin, Germany). For control experiments, a truncated form of C-domain mACE (without the N-terminal part of the molecule) was produced according to Wei et al. (1991).

2.4. Generation of cell lines expressing somatic mACE and mACE mutants

Chinese hamster ovary (CHO) cells were cultured in Ham's F-12 culture medium (Invitrogen GmbH, Karlsruhe, Germany) supplemented with 100 units/ml penicillin, 100 μg/ml streptomycin and 10% (v/v) foetal bovine serum, at 37 °C with 5% CO_2. Sixty-mm-dishes were used for transfection procedures. Using lipofectamin 2000 (Invitrogen GmbH, Karlsruhe, Germany), 7.5 μg of DNA was introduced to nearly confluent cells according to the protocol from the manufacturer. For stable transfection, selection was performed in normal growth medium containing 0.8 mg/ml G418 (Merck, Darmstadt, Germany).

The resulting three forms of ACE stably transfected into CHO cells and their corresponding membrane preparations were named as follows: for full active ACE, wtmACE; for only C-domain active mACE (N-domain is inactivated), C-domain mACE; for only N-domain active mACE (C-domain is inactivated), N-domain mACE. The correct protein expression was conformed by Western blotting (see Fig. 2B).

2.5. Screening clones on ACE activity

Enzyme activities were measured using the C-domain specific ACE substrate Hip-His-Leu and the ACE substrate (Z)-Phe-His-Leu, which is equally degraded by both ACE-domains (Danilov et al., 1994). The resulting His-Leu was coupled with *o*-phthalaldehyde as described in detail (Friedland and Silverstein, 1976; Maul et al., 2001). Fluorescence was measured in a Perkin-Elmer LS-5 spectrofluorometer. In order to control the presence of the respective mutation, we calculated the ratio of His-Leu formation from (Z)-Phe-His-Leu and from Hip-His-Leu for each of the selected clones according to Danilov et al. (1994).

Furthermore, the HPLC-monitored degradation of AcSDKP was used for final evaluation of the selected cell clones of N-domain mACE according to Rousseau et al. (1995). The hydrolysis assay conditions for AcSDKP (25 μM) were 50 mM Tris buffer, 10 μM $ZnSO_4$, pH 6.5, 37 °C. The specificity of all ACE assays was confirmed by suppression of reactions with the specific ACE inhibitor Lisinopril (10 μM) (see Fig. 2C).

We applied *t*-tests to evaluate the differences for the degradation of the used domain-selective substrates (AcSDKP and Hip-His-Leu) comparing the activities of N- and C-domain mACE-transfected cells.

2.6. Preparation of the cell homogenates and membranes

Confluent cells were harvested, washed twice with culture medium without any additives and were then centrifuged at 3000 g for 5 min at room temperature. The resulting pellets were resuspended in homogenization buffer (50 mM Tris, pH 7.5), and cells were homogenized by a glass-teflon potter (20×1100 rev/min) in an ice-bath. Thereafter, the homogenates were ultrasonicated (Bandelin-Sonopuls, Berlin, Germany) on ice, followed by centrifugation at 4 °C and 40,000 g for 22 min. The pellets were resuspended with 50 mM

Tris buffer, incubated for 30 min at 25 °C and then centrifuged again. Finally, the pellet was resuspended in 50 mM Tris buffer and stored until usage at −80 °C. Before usage all rethawed probes were ultrasonicated at 4 °C.

2.7. Degradation studies of Aβ by ACE or membrane preparations

mAβ (4–15) or hAβ (4–15) were dissolved in sterile water to 2 mM. mAβ (1–40) and hAβ (1–40) were dissolved in dimethyl sulfoxide (DMSO) to form stock solutions (2 mM). The different forms of membrane-bound mACE were incubated with 20 µl of 50 µM mAβ (1–40) in Tris buffer (pH 8.3, containing 800 mM NaCl) at 37 °C overnight. The hydrolysis assay conditions for mAβ (4–15) and hAβ (4–15) (10 µM) were 50 mM Tris buffer, 150 mM NaCl, 10 µM $ZnSO_4$, pH 7.5, 37 °C. Specificity of ACE assays was confirmed by applying the inhibitor Lisinopril (10 µM).

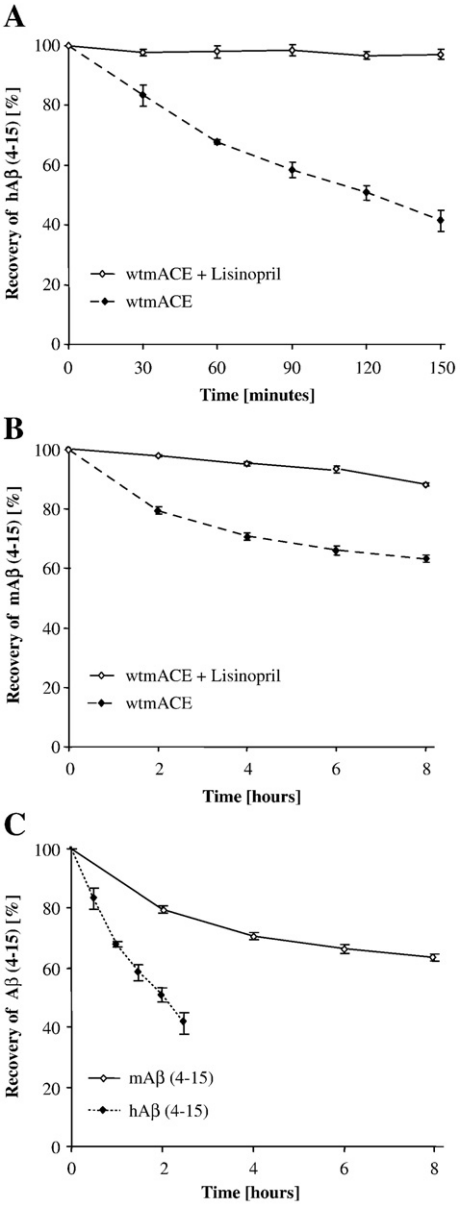

Fig. 4. HPLC-monitored Aβ (4–15) degradation studies with membrane preparations of wildtype mACE (wtmACE). The results were analyzed by two-way-ANOVA. (A) Time course of hAβ (4–15) degradation by wtmACE (dashed line) and in the presence of 10 µM Lisinopril (solid line), (n=5); mean values±S.E.M. The difference between Lisinopril inhibited and ACE-evoked degradation was $p<0.001$. (B) Time course of mAβ (4–15) degradation by wtmACE (dashed lines) and in the presence of 10 µM Lisinopril (solid line), (n=5); mean values±S.E.M. The difference between Lisinopril inhibited and ACE-evoked degradation was $p<0.001$. (C) Comparison of hAβ (4–15) (dotted line) and mAβ (4–15) (solid line) degradation. The difference between both degradation curves was $p<0.001$. For corresponding relations to Lisinopril inhibition see A and B.

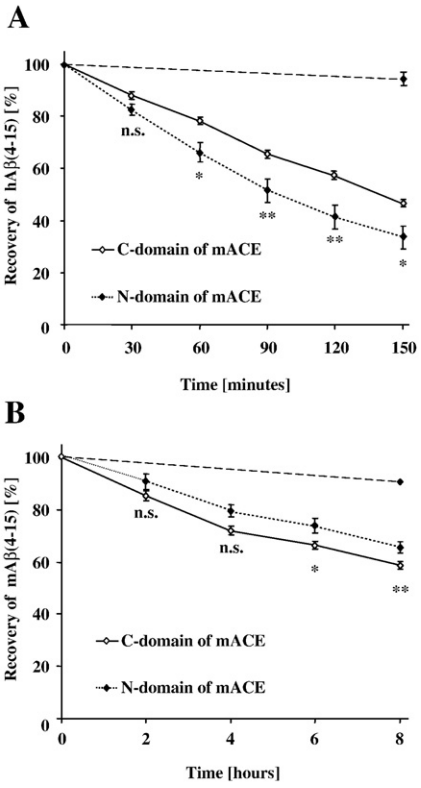

Fig. 5. Degradation of Aβ (4–15) by domain-selective mACE (solid lines, C-domain ACE; dotted lines N-domain ACE; dashed lines with filled rhombus, inhibition of ACE by 10 µM Lisinopril). The results are analyzed by two-way-ANOVA and by Bonferroni post-tests. Differences between the degradation curves and corresponding reactions in the presence of Lisinopril are always $p<0.001$. (A) Time course of hAβ (4–15) degradation by the two domains of mACE. Mean values, ±S.E.M., n=6 independent experiments. Variations among the degradation curves were significantly greater than expected by chance ($p<0.01$). Results of post-tests are indicated as n.s. = non-significant, $*p<0.05$, $**p<0.01$. (B) Time course of mAβ (4–15) degradation by the two domains of mACE. Mean values, ±S.E.M., n=6 independent experiments. Variation among the degradation curves were significantly greater than expected by chance ($p<0.01$). Results of post-tests are indicated as n.s. = non-significant, $*p<0.05$, $**p<0.01$.

Fifty µl of the reaction mixture was injected into C18 column (Shimadzu-HPLC system with UV-detection, LC10-AD, Kyoto, Japan) and eluted at 1 ml/min under isocratic conditions (86 parts of 0.1% trifluoroacetic acid, 14 parts of acetonitrile) over a period of 30 min for mAβ (4–15) and hAβ (4–15) degradation experiments. The Aβ peptides and the corresponding fragments were UV-detected at 216 nm. A linear correlation between peak areas and peptide concentration allowed quantitative analyses. All results of time dependent degradation were analyzed by two-way-ANOVA and by Bonferroni post-tests. The HPLC eluates (peaks) were collected and used for further analyses.

2.9. Matrix-Assisted Laser Desorption/Ionization Time-of-flight Mass Spectrometry (MALDI-TOF/MS)

Cleavage assays of Aβ (1–40) and recombinant ACE were set up as described above. Thirty µl of the resulting incubation solutions was

Table 1
Degradation of murine Aβ (4–15) by different forms of mACE

Forms of mACE	Measured	Calculated	Δ mass (Daltons)	Peptide	Position (counted)	Cleavage site in Aβ
N-domain mACE	895.279	895.352	0.079	FGHDSGFE(V)	1–8	$G1u^{11}$-$Va1^{12}$
C-domain mACE	895.285	895.358	0.073	FGHDSGFE(V)	1–8	$G1u^{11}$-Val^{12}
recombinant mACE	895.351	895.358	0.007	FGHDSGFE(V)	1–8	$G1u^{11}$-Val^{12}
wtmACE	895.389	895.358	−0.030	FGHDSGFE(V)	1–8	$G1u^{11}$-Val^{12}

The molecular weight of mAβ (4–15) is 1415.6 g/mol.
Degradation of mAβ (4–15) by mACE. Molecular masses, identified sequences and cleavage sites in mAβ (4–15).
mAβ (4–15) was degraded with different forms of mACE and separated by HPLC as described in detail under Materials and methods. Main degradation peaks were collected and analyzed by mass spectrometry.

purified using 10-μl pipette tips loaded with a C18 resin (ZipTip, Millipore Corporation, City, USA) according to the protocol of the manufacturer. For MALDI-MS analysis, peptides were eluted from ZipTip using step gradient elution with water/acetonitrile (10%, 30%, 50%) containing 0.1% trifluoroacetic acid (TFA). The eluates were loaded onto the MALDI plate with matrix solution (cyano-4-hydroxycinnamic acid in water/acetonitrile [2:1] containing 0.1% TFA).

MALDI-TOF/MS acquisition was performed on a Voyager STR mass spectrometer (Applied Biosystems, USA) set to reflection mode. Monoisotopic peptide masses were searched against the theoretical peptide masses of all human proteins in the Swiss-Prot and TrEMBL protein databases. MALDI-MS spectra were calibrated using several peaks as external standards. LC/MS/MS was carried out as described in detail by Korbel et al. (2005).

3. Results

As mentioned, mAβ, in contrast to hAβ, has a strongly limited tendency to form aggregated and deposed polymolecular structures (Vaughan and Peters, 1981). We here compared the formation of aggregated structures of full-length h- and mAβ (1–42) under in-vitro conditions close to physiological conditions. The final electron-microscopic visualization confirmed the difference between the two species. Unequivocal fibril formations of hAβ (see arrows) contrast with the complete absence of similar structures with mAβ (Fig. 3).

In a first degradation experiment we compared the catabolism of the N-terminal Aβ sequences mAβ (4–15) and hAβ (4–15) (see Fig. 1) by fully active wtmACE. The results of the HPLC-monitored degradation studies (decrease of areas under the peaks) are summarized in Fig. 4A and B. Lisinopril, the water-soluble, most active ACE inhibitor almost completely inhibited the peptide degradation and no additional peaks appeared in the chromatogram. This underlines the specificity of the ACE-evoked Aβ degradation. All other tested specific peptidase inhibitors were completely ineffective. Interestingly, the human form of Aβ (4–15) was much more rapidly degraded than the corresponding murine form (a time-adjusted comparison of the degradation curves is shown in Fig. 4C). HPLC eluates (peaks) were collected and used for further analysis (see below).

In a second set of experiments, we compared both domain-selective forms of mACE, C-domain mACE and N-domain mACE concerning their h- or mAβ (4–15)-hydrolyzing abilities. Domain-selective mACE mutants were derived from a wildtype ACE-clone as described in the Methods section and tested for adequate activity after transfection in CHO cells (Fig. 2B and C). In the subsequent studies on catabolism, the degradation rate of hAβ (4–15) was again much higher than that of mAβ (4–15) (Fig. 5A and B) and Lisinopril completely inhibited peptide degradation. Most interestingly, there was no obvious difference in the effectiveness of the N- and C-domain-specific forms of mACE in degrading either of the Aβ peptides. HPLC eluates (peaks) were collected and used for further analysis (see below).

The eluates from Aβ degradations were subjected to MALDI-TOF/MS. Although ACE is considered to be a dipeptidyl-carboxypeptidase, the amino acid sequence mAβ (4–13) was not detectable. However, the analysis revealed that all three forms of mACE used the same cleavage site at Glu^{11}-Val^{12} of mAβ (4–15). Thus both domains of mACE as well as the wtmACE caused endopeptidolytic cleavage of mAβ (4–15) and act on the same cleavage site (Table 1). In a parallel experiment, the amino acid sequences of the isolated peptides were analyzed by MSMS. The data confirmed the result from MALDI-TOF/MS.

We found an analogous cleavage site (Glu^{11}-Val^{12}) for hAβ (4–15), however we also observed the typical dipeptidyl-carboxypeptidase activity for ACE, as in the human N-terminal Aβ fragment the His^{13}-His^{14} bond was cleaved (Table 2). This critical difference between mAβ and hAβ degradation may result from the difference in the amino acid sequence at position 13–14 (His-His versus His-Arg) (see Figs. 1 and 6).

The above described cleavage sites of hAβ (4–15) [Glu^{11}-Val^{12} and His^{13}-His^{14}] and of mAβ (4–15) [Glu^{11}-Val^{12}] were confirmed in control experiments with soluble, recombinant mACE (R&D systems, Wiesbaden-Nordenstadt, Germany) (Tables 1 and 2).

Our results are in clear contrast to Hu et al. (2001) who described cleavage at position Asp^{7}-Ser^{8}. As mentioned above, the N-terminal

Table 2
Degradation of human Aβ (4–15) by different forms of mACE

Forms of mACE	Measured	Calculated	Δ mass (Daltons)	Peptide	Position (counted)	Cleavage sites in Aβ
N-domain mACE	1246.5939	1246.560	−0.034	FRHDSGYEVH(H)	1–10	His^{13}-His^{14}
	1010.4665	1010.433	−0.033	FRHDSGYE(V)	1–8	$G1u^{11}$-$Va1^{12}$
C-domain mACE	1246.5657	1246.560	0.000	FRHDSGYEVH(H)	1–10	His^{13}-His^{14}
	1010.4320	1010.433	−0.006	FRHDSGYE(V)	1–8	$G1u^{11}$-$Va1^{12}$
recombinant mACE	1246.610	1246.560	−0.050	FRHDSGYEVH(H)	1–10	His^{13}-His^{14}
	1010.3866	1010.433	−0.050	FRHDSGYE(V)	1–8	$G1u^{11}$-$Va1^{12}$
wtmACE	1010.447	1010.433	−0.014	FRHDSGYE(V)	1–8	$G1u^{11}$-$Va1^{12}$

The molecular weight of hAβ (4–15) is 1511.6 g/mol.
Degradation of hAβ (4–15) by mACE. Molecular masses, identified sequences and cleavage sites in hAβ (4–15).
hAβ (4–15) was degraded with different forms of mACE and separated by HPLC as described in detail under Materials and methods. Main degradation peaks were collected and analyzed by mass spectrometry.

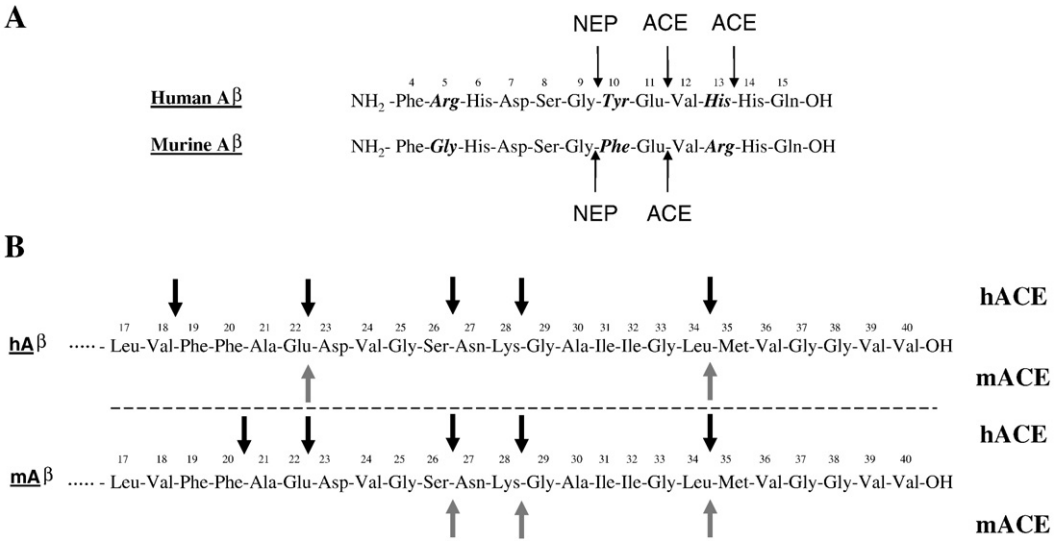

Fig. 6. Amino acid sequences of hAβ- and mAβ-fragments and cleavage sites by ACE degradation. Species-specific amino-acid differences are indicated in bold and Italics. Found cleavage sites are indicated by arrows. Summary of the results presented in Tables 1–4. (A) Amino acid sequences of hAβ (4–15) and mAβ (4–15). Peptidolytic attacks by membrane-bound mACE and NEP are indicated by arrows. (B) Amino acid sequences of hAβ (1–40) and mAβ (1–40). Peptidolytic attacks by recombinant mACE or hACE are indicated by arrows.

part of mAβ keeps three distinct sequential modifications in comparison to human Aβ, but these differences do not relate to the newly identified main cleavage site of ACE (Glu^{11}-Val^{12}). Moreover, our results are somewhat in contrast to those of Oba et al. (2005), because they reported that the N-domain of human ACE degraded amyloid amyloid-β peptide much more effective. Statistical calculations demonstrate that there are still some differences between both domain-selective forms of mACE in our experiments. But these differences become significant only after long-time incubations (see Fig. 5), these differences are incommensurate with the great differences in the degradation curves in Fig. 4, and they are quite non-uniform concerning the both substrates (mAβ[4–15] versus hAβ[4–15]). We conclude that there is no domain-selectivity in the degradation of Aβ by mACE.

The here described cleavage sites differ from that Hu et al. (2001) found in full-length hAβ hydrolysis (Asp^7-Ser^8 cleavage) by hACE. Thus, we repeated our degradation experiments with hAβ (1–40) in order to exclude that the cleavage site at Asp^7-Ser^8 may have disappeared using the shorter fragment. Because of the very slow degradation with full-length Aβ, we abstained from time dependent degradation curves. To investigate the cleavage sites of the full-length Aβ after long-time incubations with recombinant hACE or mACE, respective gradient eluates from C18 ZipTip were analyzed by MALDI-TOF/MS. Our results are summarized in the Tables 3 and 4 (see also Fig. 6B). All found cleavage sites are localized in the completely uniform C-terminal part of the both Aβ molecules and all the identified degradation products were not detectable in the presence of the specific ACE inhibitor Lisinopril. Obviously, the resulting products are a mixture of endopeptidolytic and subsequent dipeptidolytic hydrolysis. In all four variants, the Aβ position 34–35 (Leu-Met) was endopeptidolytically attacked by ACE. There seem to be further endopeptidolytic cleavage sites at positions 28–29 (Lys-Gly) and 22–23 (Glu-Asp). After these initial endopeptidolytic cleavages, dipeptidolytic activities obviously result in the formation of the corresponding shorter molecules, like Aβ (1–26), Aβ (1–20), Aβ (1–18). Aβ (1–18) was the shortest detectable molecule. Although the molecule Aβ (1–20) was exclusively found in hAβ degradation by hACE, we can not exclude that again dipeptidolytic activities result in the stepwise formation of shorter molecules up to Aβ (1–18). Notably, corresponding C-terminal cleavage products (beginning with Aβ[35–40]) were not detected.

Table 3
Degradation of Aβ (1–40) by recombinant mACE

Measured	Calculated	Δ mass (Daltons)	Peptide	Position (counted)	Cleavage site in Aβ
A. Degradation of murine Aβ (1–40) by recombinant mACE					
3689.976	3689.835	0.141	DAEFGHDSGFEVRHQKLVFFAEDVGSNKGAIIGL(M)	1–34	Leu^{34}-Met^{23}
2565.2473	2565.216	−0.031	DAEFGHDSGFEVRHQKLVFFAE(D)	1–22	Glu^{22}-Asp^{23}
The molecular weight of mAβ (1–40) is 4232.123 g/mol.					
mAβ (1–40) was degraded with recombinant mACE, purified using C18-loaded ZipTips and analyzed with MALDI-TOF/MS.					
B. Degradation of human Aβ (1–40) by recombinant mACE					
3786.2268	3785.8669	0.360	DAEFRHDSGYEVHHQKLVFFAEDVGSNKGAIIGL(M)	1–34	Leu^{34}-Met^{35}
3261.6870	3261.5347	0.152	DAEFRHDSGYEVHHQKLVFFAEDVGSNK(G)	1–28	Lys^{28}-Gly^{29}
3019.5350	3019.3968	0.138	DAEFRHDSGYEVHHQKLVFFAEDVGS(N)	1–26	Ser^{26}-Asn^{27}
The molecular weight of hAβ (1–40) is 4328.1556 g/mol.					
hAβ (1–40) was degraded with recombinant mACE, purified using C18-loaded ZipTips and analyzed with MALDI-TOF/MS.					

Molecular masses, identified sequences and cleavage sites in Aβ (1–40).

Table 4
Degradation of Aβ (1–40) by recombinant hACE

Measured	Calculated	Δ mass (Daltons)	Peptide	Position (counted)	Cleavage site in Aβ
A. Degradation of murine Aβ (1–40) by recombinant hACE					
3689.535	3689.835	−0.300	DAEFGHDSOFEVRHQ KLVF FAEDVOSNKGAII GL(M)	1–34	Leu^{34}-Met^{35}
3165.650	3165.502	0.148	DAEFGHDSOFEVRHQ KLV F FAEDVO SNK(G)	1–28	Lys^{28}-$G1y^{29}$
2923.526	2923.364	0.162	DAEFGHDSOFEVRHQ KLV F FAEDVO 3(N)	1–26	Ser^{26}-Asn^{27}
2565.433	2565.216	0.217	DAEFOHDSOFEVRHQ KLV F FAE(D)	1–22	$G1u^{22}$-Asp^{23}
2071.1477	2070.999	0.149	DAE FGHDSOFEVRHQ KLV (F)	1–18	Vul^{18}-Phe^{19}
The molecular weight of mAβ (1–40) is 4232.123 g/mol.					
mAβ (1–40) was degraded with recombinant hACE, purified using C18-loaded ZipTips and analyzed with MALDI-TOF/MS.					
B. Degradation of human Aβ (1–40) by recombinant hACE					
3785.8795	3785.8669	0.013	DAEFRHDSGYEV HHQ KLVF FAEDVGSNKGAII GL(M)	1–34	Leu^{34}-Met^{35}
3261.3964	3261.5347	−0.138	DAEFRHDSGYEV HHQ KLVF FAEDVGSNK(G)	1–28	Lys^{28}-$G1y^{29}$
3019.370	3019.3968	−0.027	DAEFRHDSGYEV HHQ KLVF FAEDVOS(N)	1–26	Ser^{26}-Asn^{27}
2661.1691	2661.248	−0.079	DAEFRHDSGYEV HHQ KLVF FAE(D)	1–22	Glu^{22}-Asp^{23}
2461.1205	2461.1683	−0.048	DAEFRHDSGYEVHHO KLVF F(A)	1–20	Phe^{20}-Ala^{21}
The molecular weight of hAβ (1–40) is 4328.1556 g/mol.					
hAβ (1–40) was degraded with recombinant hACE, purified using C18-loaded ZipTips and analyzed with MALDI-TOF/MS.					

Molecular masses, identified sequences and cleavage sites in Aβ (1–40).

Obviously, these peptides are rapidly degraded by ACE. In spite of an intensive search, molecules originating from cleavage at Asp^{7}-Ser^{8} were not found.

4. Discussion

As mentioned, only three amino acid residues localized in the N-terminal parts of h- and mAβ are responsible for all the known differences between these peptides. These differences are most interesting, since rats and mice do not develop an Alzheimer-like neuropathology with advancing age. Both biophysical and chemical properties of the peptides might be responsible for these dramatic differences. Our in-vitro aggregation studies summarized in Fig. 3 show fibril formations with hAβ and the complete absence of corresponding macromolecular structures with a parallel sample of mAβ. On the other hand, our data also revealed that there are definite biochemical differences, e.g. in the enzymatic degradability of the two molecules (see Fig. 4C).

NEP as well as ACE are described to hydrolyze hAβ in its N-terminal region (Hu et al., 2001; Iwata et al., 2000). Whereas the cleavage by NEP is expected because of the prominent cleavage site at Gly^{9}-Tyr^{10} (NEP generally cleaves at the N-terminal site of hydrophobic amino acids), the endopeptidolytic action of ACE on hAβ (Asp^{7}-Ser^{8}) as described by Hu et al. (2001) was a most astonishing finding. Consequently, the aim of this study was to analyze the action of ACE on the structurally differing N-terminal parts of h- and mAβ. Moreover, we wanted to examine whether or not both catalytic domains of ACE are involved in the cleavage of Aβ. The two domains are known to play non-uniform roles in catabolic processes (Deddish et al., 1998; Araujo et al., 2000; Rice et al., 2004). In the present study, we focused on the degradation of the N-terminal sequences Aβ (4-15), which include the three distinct amino acid exchanges between h- and mAβ as well as the above described cleavage sites. Moreover, by using these truncated forms of Aβ for HPLC-monitored degradation studies, we avoided problems with solubility and spontaneous formation of multimeric structures and associates.

First of all, we confirmed that ACE, generally known as a dipeptidyl-carboxy-peptidase, exerts an endopeptidolytic attack on the N-terminal sequence Aβ (4–15) as well as on the full-length molecule Aβ (1–40). All forms of ACE were found to be not very effective in the cleavage of full-length Aβ. This is in agreement with Eckman et al. (2006), who described that ACE does not substantially influence the steady state of central Aβ-levels. Nevertheless, in our studies a detectable degradation of full-length Aβ occurred after long-time incubation with recombinant ACE. With full-length Aβ, the smallest detectable peptide among the degradation products was Aβ (1–18). Aβ degradation in all of the ACE forms was always completely inhibitable by Lisinopril, a specific inhibitor of ACE. This excludes that any contaminations with other peptidases are responsible for the observed degradations. In contrast to full-length Aβ, both Aβ (4–15) molecules – human and murine – were effectively hydrolyzed by all forms of ACE at position Glu^{11}-Val^{12}. hAβ (4–15) was also hydrolyzed at His^{13}-His^{14}. These results in truncated Aβ confirm Hu et al. (2001) with respect to an ACE-caused endopeptidolytic action on Aβ, but contradict their paper with regard to the described cleavage of hAβ between $Asp^{7}$and Ser^{8} (see below).

The ability of the two catalytic domains of ACE to degrade Aβ is controversially discussed (Hu et al., 2001; Hemming and Selkoe, 2005; Oba et al., 2005). We found that Aβ (4–15) is cleaved with a similar effectiveness by both domains of mACE. This result does not support previous findings of Oba et al. (2005) that exclusively the N-domain of ACE was able to degrade hAβ. The difference between the two studies may result from the different forms of mutation to generate the domain-specific clones. In our present study, both the N- and C-domains of mACE were derived from a full-length clone by inactivating the catalytic centers with point-mutations (His/Lys). Consequently, the three-dimensional structure should be widely unchanged in our mutated ACE forms.

The curves of the degradation of Aβ (4–15) by the three forms of mACE (Figs. 4 and 5) indicate that the total activity of mACE is not the sum of the activities of the two catalytic domains. We conclude that the two active sites of mACE influence each other; and we postulate that there is negative cooperation between the two domains. Negative cooperativity has already been described for the hydrolytic activity of both domains of bovine ACE using standard ACE substrates (Binevski et al., 2003).

Surprisingly, all identified cleavage sites in the *full-length* Aβ molecule are localized in the uniformly structured C-terminal part of Aβ. In spite of intensive search, molecules that should originate from an Asp^{7}-Ser^{8} cleavage in the N-terminal part, as it was suggested by Hu et al. (2001), were not detectable. We suppose that the degradation in our experiments are mixtures of endopeptidolytic and subsequent dipeptidolytic attacks of ACE. Endopeptidolytic cleavage sites are found at positions 34–35 (Leu-Met), 28–29 (Lys-Gly), and 22–23 (Glu-Asp). Exclusively long N-terminal Aβ-fragments were identified among the degradation products, while corresponding C-terminal cleavage products did not occur. Probably, the latter peptides were rapidly catabolized by ACE.

In spite of five additional cleavage sites identified after interaction with hACE, there is no clear evidence for different degradation profiles. Using mACE we always identified cleavage sites which altogether are known from our degradations with hACE. We initiated our studies always with the same, exactly adjusted ACE activity. But we can not exclude that the greater number of identified Aβ degradation products is a reflection of a greater stability of the used hACE charges under our experimental conditions.

The general importance of ACE in Alzheimer's disease has been discussed in genetic studies on humans. These studies revealed that

ACE gene polymorphism [an insertion (*I*)/deletion (*D*) within intron 16] associates with Alzheimer's disease. The *D* allele is associated with high ACE activity and Alzheimer's disease protection, whereas the *I* allele is associated with low ACE activity (Morris et al., 1994; Jalil et al., 2004) and an increased risk in Alzheimer's disease (Rigat et al., 1990; Kehoe et al., 1999; Yang et al., 2000a,b). In addition, a selective alteration in ACE density was shown in the human cortex of patients with Alzheimer's disease (Barnes et al., 1991).

As mentioned, rats and mice do not develop the typical forms of Alzheimer-like neuropathology with advancing age (Liu et al., 1999; Yang et al., 2000a,b; Bush, 2003). This specificity is not completely understood; besides the different peptidolytic attacks discussed here (see Fig. 4C), also metal ion- (esp. Zn^{++} or Cu^{++}) induced aggregations and precipitations are found to be different between h- and mAβ (Bush et al., 1994; Atwood et al., 1998). Interestingly, the N-terminal part of Aβ plays a crucial role in these processes as well. Liu et al. (1999) and Zirah et al. (2006) identified the residues His^6, His^{13}, His^{14} and the Glu^{11} as ligands that coordinate Zn^{2+}. In the light of these findings, our results on ACE-evoked cleavage in the N-terminal part of Aβ at the positions Glu^{11}-Val^{12} and His^{13}-His^{14} could be of special importance.

We also analyzed the h- or mAβ (4–15) catabolism with recombinant NEP by HPLC and subsequent MALDI-TOF/MS. In that case we unequivocally confirmed the published cleavage site within the Aβ molecule (Howell et al., 1995; Iwata et al., 2000; Yasojima et al., 2001) at Gly^9-Tyr^{10} rsp. Gly^9-Phe^{10} (data not shown).

Summarizing our results, we describe for the first time the ACE-evoked hydrolysis of the N-terminal part of m- and hAβ. We confirm that there are indeed endopeptidolytic attacks of ACE on Aβ peptides. Surprisingly, both catalytic domains of ACE were found to be similarly involved in the Aβ catabolism. On the other hand, when we compared the ACE-evoked degradation of m- and hAβ, we found different catabolism rates and different cleavage sites. The N-terminal part of Aβ is structurally most important because it contains the three different amino acids between hAβ and mAβ; moreover, this part of Aβ contains the functionally most relevant zinc-binding site of the molecule. Consequently, all hydrolytic attacks on this part of Aβ should be of exceptional interest.

Acknowledgements

We are most grateful to Bettina Kahlich as well as Jenny Eichhorst for expert technical assistance.

References

Araujo, M.C., Melo, R.L., Cesari, M.H., Juliano, M.A., Juliano, L., Carmona, A.K., 2000. Peptidase specificity characterization of C- and N-terminal catalytic sites of angiotensin I-converting enzyme. Biochemistry 39, 8519–8525.

Atwood, C.S., Moir, R.D., Huang, X., Scarpa, R.C., Bacarra, N.M., Romano, D.M., Hartshorn, M.A., Tanzi, R.E., Bush, A.I., 1998. Dramatic aggregation of Alzheimer Ab by Cu II is induced by conditions representing physiological acidosis. J. Biol. Chem. 273, 12817–12826.

Barnes, N.M., Cheng, C.H., Costall, B., Naylor, R.J., Williams, T.J., Wischik, C.M., 1991. Angiotensin converting enzyme is increased in temporal cortex from patients with Alzheimer's disease. Eur. J. Pharmacol. 200, 289–292.

Binevski, P.V., Sizova, E.A., Pozdnev, V.F., Kost, O.A., 2003. Evidence for the negative cooperativity of the two active sites within bovine somatic angiotensin-converting enzyme. FEBS Letters, 550, 84–88.

Bush, A.I., Pettingell, W.H., Multhaup, G., d Paradis, M., Vonsattel, J.P., Gusella, J.F., Beyreuther, K., Masters, C.L., Tanzi, R.E., 1994. Rapid induction of Alzheimer Ab amyloid formation by zinc. Science 265, 1464–1467.

Bush, A.I., 2003. The metallobiology of Alzheimer's disease. Trends Neurosci. 26, 207–214.

Chauhan, N.B., Siegel, G.J., 2005. Efficacy of anti-Aβ antibody isotypes used for intracerebroventricular immunization in TgCRND8. Neurosci. Lett. 375, 143–147.

Danilov, S., Jaspard, E., Churakova, T., Towbin, H., Savoie, F., Wei, L., Alhenc-Gelas, F., 1994. Structure-function analysis of angiotensin I-converting enzyme using monoclonal antibodies. Selective inhibition of the amino-terminal active site. J. Biol. Chem. 269, 26806–26814.

Deddish, P.A., Marcic, B., Jackman, H.L., Wang, H.Z., Skidgel, R.A., Erdos, E.G., 1998. N-domain-specific substrate and C-domain inhibitors of angiotensin-converting enzyme angiotensin-1–7 and keto-ACE. Hypertension 31, 912–917.

Eckman, E.A., Adams, S.K., Troendle, F.J., Stodola, B.A., Kahn, M.A., Fauq, A.H., Xiao, H.D., Bernstein, K.E., Eckman, C.B., 2006. Regulation of steady-state beta-amyloid levels in the brain by neprilysin and endothelin-converting enzyme but not angiotensin-converting enzyme. J. Biol. Chem. 281, 30471–30478.

Friedland, J., Silverstein, E., 1976. A sensitive fluorimetric assay for serum angiotensin-converting enzyme. Amer. J. Clin. Pathol. 66, 416–424.

Hardy, J., Selkoe, D.J., 2002. The amyloid hypothesis of Alzheimer's disease, progress and problems on the road to therapeutics. Science 297, 353–356.

Hemming, M.L., Selkoe, D.J., 2005. Amyloid β-protein is degraded by cellular angiotensin-converting enzyme ACE and elevated by an ACE inhibitor. J. Biol. Chem. 280, 37644–37650.

Howell, S., Nalbantoglu, J., Crine, P., 1995. Neutral endopeptidase can hydrolyze beta-amyloid 1-40 but shows no effect on beta-amyloid precursor protein metabolism. Peptides 16, 647–652.

Hu, J., Igarashi, A., Kamata, M., Nakagawa, H., 2001. Angiotensin-converting enzyme degrades Alzheimer amyloid β-peptide Aβ; retards Aβ aggregation, deposition, fibril formation; and inhibits cytotoxicity. J. Biol. Chem. 276, 47863–47868.

Iwata, N., Tsubuki, S., Takaki, Y., Watanabe, K., Sekiguchi, M., Hosoki, E., Kawashima-Morishima, M., Lee, H.J., Hama, E., Sekine-Aizawa, Y., Saido, T.C., 2000. Identification of the major Abeta1-42-degrading catabolic pathway in brain parenchyma, suppression leads to biochemical and pathological deposition. Nat. Med. 6, 143–150.

Jalil, J.E., Ocaranza, M.P., Oliveti, C., Cordova, S., Godoy, I., Chamorro, G., Braun, S., Fardella, C., Michel, J.B., Lavandero, S., 2004. Neutral endopeptidase and angiotensin I converting enzyme insertion/deletion gene polymorphism in humans. J. Hum. Hypertens. 18, 119–125.

Janek, K., Behlke, J., Zipper, J., Fabian, H., Georgalis, Y., Beyermann, M., Bienert, M., Krause, E., 1999. Water-soluble beta-sheet models which self-assemble into fibrillar structures. Biochemistry 38, 8246–8252.

Jaspard, E., Wie, L., Alhenc-Gelas, F., 1993. Differences in the properties and enzymatic specificities of the two active sites of angiotensin I-converting enzyme kininase 11. J. Biol. Chem. 268, 9496–9503.

Kehoe, P.G., Russ, C., McIlory, S., Williams, H., Holmans, P., Holmes, C., Liolitsa, D., Vahidassr, D., Powell, J., McGleenon, B., Liddell, M., Plomin, R., Dynan, K., Williams, N., Neal, J., Cairns, N.J., Wilcock, G., Passmore, P., Lovestone, S., Williams, J., Owen, M.J., 1999. Variation in DCP1, encoding ACE, is associated with susceptibility to Alzheimer disease. Nat. Gen. 21, 71–72.

Korbel, S., Schumann, M., Bittorf, T., Krause, E., 2005. Relative quantification of erythropoietin receptor-dependent phosphoproteins using in-gel ^{18}O-labeling and tandem mass spectrometry. Rapid Commun. Mass. Spectrom. 19, 2259–2271.

Kozin, S.A., Zirah, S., Rebuffat, S., Hoa, G.H., Debey, P., 2001. Zinc binding to Alzheimer's Abeta 1–16 peptide results in stable soluble complex. Biochem. Biophys. Res. Commun. 285, 959–964.

Liu, S.T., Howlett, G., Barrow, C.J., 1999. Histidine-13 is a crucial residue in the zinc Ion-induced aggregation of the Aβ peptide of Alzheimer's disease. Biochemistry 38, 9373–9378.

Maul, B., Siems, W.E., Hoehe, M.R., Grecksch, G., Bader, M., Walther, T., 2001. Alcohol consumption is controlled by angiotensin II. FASEB J. 15, 1640–1642.

Miura, T., Suzuki, K., Kohata, N., Takeuchi, H., 2000. Metal binding modes of Alzheimer's amyloid, peptide in insoluble aggregates and soluble complexes. Biochemistry 39, 7024–7031.

Mohajeri, M.H., Gaugler, M.N., Martinez, J., Tracy, J., Li, H., Crameri, A., Kuehnle, K., Wollmer, M.A., Nitsch, R.M., 2004. Anti-amyloid activity of neprilysin in plaque-bearing mouse models of Alzheimer's disease. FEBS Lett. 562, 16–21.

Morris, B.J., Zee, R.Y., Schrader, A.P., 1994. Different frequencies of angiotensin-converting enzyme genotypes in older hypertensive individuals. J. Clin. Invest. 94, 1085–1089.

Oba, R., Igarashi, A., Kamata, M., Nagata, K., Takano, S., Nakagawa, H., 2005. The N-terminal active centre of human angiotensin-converting enzyme degrades Alzheimer amyloid β-peptide. Europ. J. Neurosci. 21, 733–740.

Rice, G.I., Thomas, D.A., Grant, P.J., Turner, A.J., Hooper, N.M., 2004. Evaluation of angiotensin-converting enzyme ACE, its homologue ACE2 and neprilysin in angiotensin peptide metabolism. Biochem. J. 383, 45–51.

Rigat, B., Hubert, C., Alhenc-Gelas, F., Cambien, F., Corvol, P., Soubrier, F., 1990. An insertion/deletion polymorphism in the angiotensin I-converting enzyme gene accounting for half the variance of serum enzyme levels. J. Clin. Invest. 86, 1343–1346.

Rousseau, A., Michaud, A., Chauvet, M.T., Lenfant, M., Corvol, P., 1995. The hemoregulatory peptide *N*-Acetyl-Ser-Asp-Lys-Pro is a natural and specific substrate of the N-terminal active site of human angiotensin-converting enzyme. J. Biol. Chem. 270, 3656–3661.

Saido, T.C., Iwata, N., 2006. Metabolism of amyloid beta peptide and pathogenesis of Alzheimer's disease. Towards presymptomatic diagnosis, prevention and therapy. Neurosci. Res. 54, 235–253.

Vaughan, D.W., Peters, A., 1981. The structure of neuritic plaque in the cerebral cortex of aged rats. J. Neuropathol. Exp. Neurol. 40, 472–487.

Wang, D.S., Dickson, D.W., Malter, J.S., 2006. β-Amyloid degradation and Alzheimer's disease. J. Biomed. Biotechnol. 2006, 58406-5807.

Wei, L., Alhenc-Gelas, F., Corvol, P., Clauser, E., 1991. The two homologous domains of human angiotensin I-converting enzyme are both catalytically active. J. Biol. Chem. 266, 9002–9008.

Wei, L., Clauser, E., Alhenc-Gelas, F., Corvol, P., 1992. The two homologous domains of human angiotensin I-converting enzyme interact differently with competitive inhibitors. J. Biol. Chem. 267, 13398–13405.

Yang, D.S., McLaurin, J., Qin, K., Westaway, D., Fraser, P.E., 2000a. Examining the zinc binding site of the amyloid-b peptide. Eur. J. Biochem. 267, 6692–6698.

Yang, J.D., Feng, G., Zhang, J., Lin, Z.X., Shen, T., Breen, G., St Clair, D., He, L., 2000b. Association between angiotensin-converting enzyme gene and late onset Alzheimer's disease in Han Chinese. Neurosci. Lett. 295, 41–44.

Yasojima, K., Akiyama, H., McGeer, E.G., McGeer, P.L., 2001. Reduced neprilysin in high plaque areas of Alzheimer brain, a possible relationship to deficient degradation of β-amyloid peptide. Neurosci. Lett. 297, 97–100.

Zirah, S., Kozin, S.A., Mazur, A.K., Blond, A., Cheminant, M., Segalas-Milazzo, I., Debey, P., Rebuffat, S., 2006. Structural changes of region 1–16 of the Alzheimer disease amyloid β-peptide upon zinc binding and in vitro aging. J. Biol. Chem. 281, 2151–2161.